Distributed Aerodynamic Control using Active Trailing-Edge Flaps for Large Wind Turbines

Roland Feil[1], Nikhar Abbas[1,2], Pietro Bortolotti[1], Nick Johnson[1], and Ben Mertz[3]

[1] National Renewable Energy Laboratory, Boulder, CO 80303, USA
[2] University of Colorado Boulder, Boulder, CO 80309, USA
[3] Rose-Hulman Institute of Technology, Terre Haute, IN 47803, USA

E-mail: roland.feil@nrel.gov
Keywords: distributed aerodynamic control, active trailing-edge flaps, MDAO, large rotors

Abstract. This work presents a numerical framework to investigate distributed aerodynamic control devices for application in large wind turbines. Tool capabilities were extended to facilitate multiple aerodynamic polar tables. The airfoil aerodynamics characteristics were automatically determined, and blade-pitch, generator-torque, and trailing-edge-flap controllers were tuned in-the-loop according to a specific blade design. This automated workflow allows analysis and optimization of trailing-edge flaps, enabling codesign studies. Results targeted reductions of root-flap-bending moment derivatives. The applied trailing-edge-flap control reduced the standard deviation of root-flap-bending moments by more than 6% and benefit related parameters, e.g., reduce blade-tip deflections, by up to 8%. Because of varying thrust distributions along the blade span, different flap designs have nonlinear characteristics in terms of the control objective and show best performance when located at the radial position with maximum thrust. In general, larger flaps provide a greater influence to reduce the target control objective.

1. Introduction

The Big Adaptive Rotor (BAR) project, funded by the U.S. Department of Energy, seeks to enable larger land-based rotors and aims to investigate novel technologies to support the growth in turbine size and continued reduction in levelized cost of energy (LCOE) of land-based wind turbines [1]. One promising technology to enable larger rotors is using distributed aerodynamic control (DAC) devices. DAC devices can lower the loads on the rotor while serving as another mechanism to regulate power [2]. This work presents a numerical framework to conduct codesign analysis of wind turbine blades equipped with DAC devices.

The BAR project designed a baseline blade for a 5-MW turbine with a 100-m rotor blade. These machines are characterized by increasingly flexible and large rotor blades that introduce challenges in several areas. For example, with larger blades, the operational pitch rate decreases. DAC offers a technology solution to reduce blade and hub loads, power oscillations, rotor overspeeds, and load cycles to mitigate a slower pitch control system. Overall, DAC represents a promising area of research to support mitigating technical requirements that emerge with increasing rotor sizes.

Numerous research studies have examined the challenge of introducing DAC devices in

wind turbine blades [3, 4]. Both Barlas et al. [5] and Johnson et al. [6] reviewed the state-of-the-art of smart rotor control concepts, including flaps, microtabs, camber control, active twist, and boundary layer control. More recently, numerical and experimental studies have looked at morphing trailing edges [7]. In this study, rigid trailing-edge flaps were chosen as the actuator because of their well-understood performance characteristics [8] and technical readiness level compared to other DAC techniques [4]. An aerodynamic disadvantage of using flaps is the increased drag, especially at flap deflection angles above 10° [8]. Further challenges to overcome are the manufacturing complexity, cost, and reliability of DAC devices. However, their effectiveness in wind turbine applications is considered to be high for alleviating power and load fluctuations [9]. While the potential of using smart control concepts to reduce fatigue loads [10–13] and increase power production at below-rated speeds [14] has been demonstrated, few studies have been conducted using a general multidisciplinary design analysis and optimization (MDAO) approach [15, 16]. Most studies of DAC found in literature were applied to existing blade designs that were not optimized with DAC in mind, i.e. no codesign being conducted, but to achieve the full advantage of DAC devices, those should be considered into the blade design from the start [17]. Aubrun et al. [18] stressed the need for more interdisciplinary studies to be conducted that account for the many challenges that need to be overcome to successfully deploy DAC devices.

The presented work targets this gap in research by aiming to further the understanding of such control devices, assess their impact on global metrics of interest (e.g., loads reduction), and ultimately evaluate their functionality for future generations of very large wind turbine rotors. This is facilitated through novel modeling capabilities with sophisticated control strategies and development of codesign analysis metrics to assess system-wide impacts of trailing-edge flaps.

2. Modeling Approach

OpenFAST [19], an open-source aero-servo-elastic wind turbine simulation tool developed at the National Renewable Energy Laboratory (NREL), has been updated to support arbitrary DAC devices. In this study, trailing-edge flaps were used to demonstrate these modeling capability improvements, though they can be adapted to model other DAC devices, such as leading-edge flaps, microtabs, morphing concepts, and any other method that can be used to actively control the aerodynamic characteristics of an airfoil section. Additionally, a flap-control module has been included in NREL's Reference OpenSource Controller (ROSCO) [20]. Furthermore, the Wind-Plant Integrated System Design and Engineering Model (WISDEM®) [21] has been updated to add modeling and optimization capabilities for DAC devices. WISDEM now features XFoil [22] pre- and postprocessing capabilities. This enables automatic generation of aerodynamic polar tables of deflected trailing-edge flaps for arbitrary blade cross-sectional geometries during an analysis and optimization. Collectively, this provides the framework for developing wind turbine blades with optimized DAC placement and design. The combined workflow between OpenFAST, WISDEM, XFoil, and ROSCO is shown in Fig. 1. More details of each module's features are described in the following sections.

2.1. OpenFAST

OpenFAST was recently updated to include an airfoil lift, drag, and pitching-moment interpolation feature. Therefore, in addition to interpolating the aerodynamic polar tables for varied angles of attack, OpenFAST now includes the ability to interpolate another dimension, such as various Reynolds numbers or arbitrary aerodynamic modifications due to DAC devices. For the purposes of this study, this parameter was chosen to be the trailing-edge-flap deflection angle, δ_{flap}. However, OpenFAST can handle DAC devices other than trailing-edge flaps, provided that a characteristic relationship can be determined between the device's actuator input and its effect on the corresponding airfoil aerodynamics. For this study, a linear characteristic

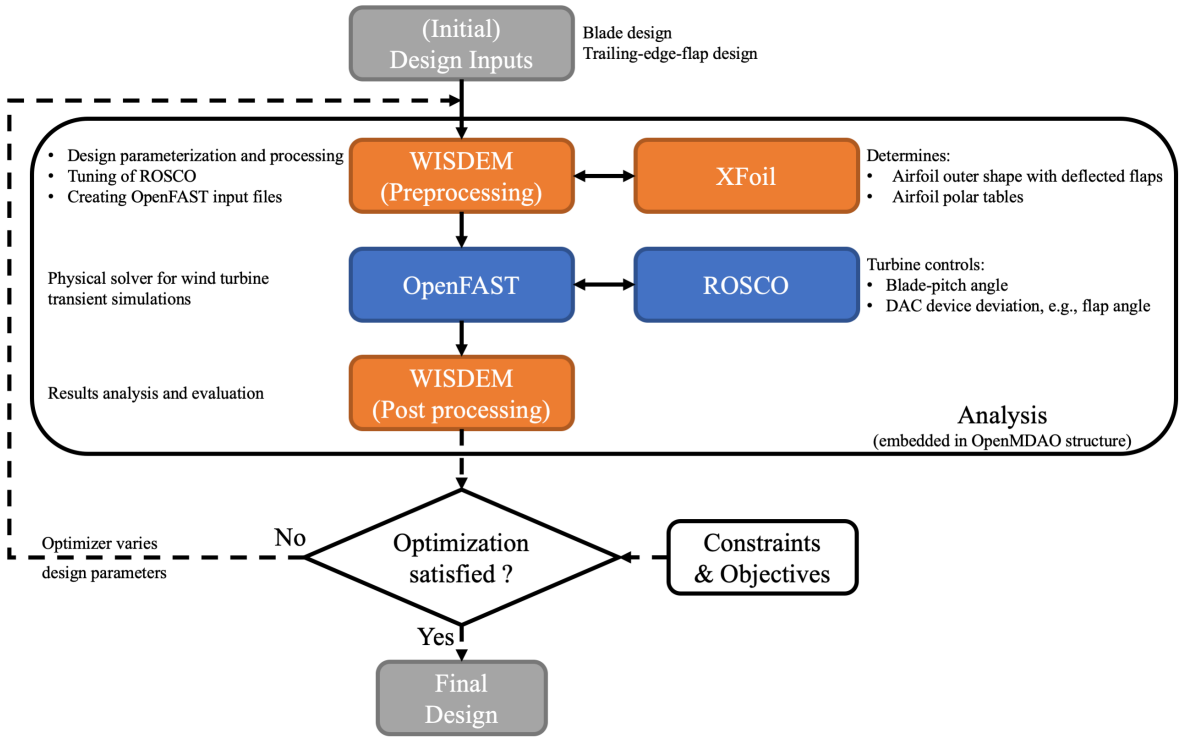

Figure 1. Modeling approach for distributed aerodynamic control analysis and optimization.

was assumed and, at each blade station that incorporates a DAC device, three different polar tables were used–minimum, neutral, and maximum trailing-edge-flap deflection angles. OpenFAST linearly interpolates between the three stations to derive the polars for a given flap-deflection angle. More tables may be added for capturing nonlinear effects.

In order to actuate the user-defined DAC device, the available user-defined input variables in the bladed-style dynamic link library are used to pass DAC control inputs to ServoDyn, the controller module and interface for OpenFAST. The ROSCO controller is used to define these control inputs (Fig. 1). Currently, each channel corresponds to a flap-deflection angle for a single blade of a three-bladed rotor with one flap per blade, allowing for each blade's flap to be controlled independently. To implement additional actuators in the future (i.e., multiple DAC devices per blade), more user-defined channels can be made available in ROSCO and ServoDyn.

2.2. WISDEM and XFoil

WISDEM is a multidisciplinary analysis and design environment for wind turbine applications. It consists of a set of modules for evaluating global metrics of performance, including LCOE. WISDEM and its independent submodules are built in the OpenMDAO framework [23]. As presented in the schematics of Fig. 1, WISDEM has the capability to load initial wind turbine designs, preprocess and parameterize the design or other physical parameters as well as generate and run OpenFAST models and process the results. Recent modifications have enabled features that generate updated AeroDyn input files for OpenFAST. The initial design inputs were extended to account for the trailing-edge flaps, including the starting and ending positions along the span, the chord coverage of the flap at the trailing edge, the minimum and maximum deflection angles, and the number of flap-deflection angles. This provides a convenient mechanism to specify and optimize the trailing-edge-flap characteristics.

Figure 2 presents the modified airfoil outer shapes and polar tables for the FFA-W3-211 airfoil. Based on the starting and ending positions of the flaps, WISDEM determines the number of airfoil tables at a specific radial station. At radial stations with flaps, XFoil is called twice. First, based on the defined flap-deflection angles, XFoil determines the deviated airfoil outer-shapes that, once generated, also undergo airfoil outer-shape smoothing using a Gaussian filter (Fig. 2(a)). Having smooth shapes at the hinge point strongly improves the convergence during the following analysis step in XFoil. Second, for each of those generated airfoil shapes, XFoil is used to determine the aerodynamic characteristics in terms of the airfoil polars (Figs. 2(b) through (d)). Thereby, XFoil is embedded into the WISDEM framework and called iteratively during the design loop (Fig. 1). Note that calling XFoil increases the computational expense within an optimization. In order to maintain consistency throughout the analysis and optimization, airfoil aerodynamic characteristics at radial stations without DAC devices were determined in the same manner (i.e., using the same XFoil settings) as radial stations that accounted for a DAC device. Consistent aerodynamics are of great importance for analyzing and optimizing blades with DAC devices.

2.3. Controller

Standard blade-pitch and generator-torque controllers are used to operate at turbine-rated rotor speed and constant generator torque, respectively. In order to support investigation of trailing-edge flaps, the ROSCO toolbox was extended to support generic proportional-integral (PI) controller tuning and implementation for DAC devices. In a feedback loop between ROSCO and OpenFAST, the additional trailing-edge-flap controller addresses the first derivative of the out-of-plane blade-root bending moments. A simplified blade model based on the airfoil aero-structural characteristics is used to tune a PI controller for a desired closed response of this signal. Additionally, the trailing-edge-flap deflection angle, δ_{flap}, is integrated to encourage the flap mean toward zero degrees. This results in a controller that aims to minimize changes in blade-root bending moments without significant drift from $\delta_{flap} = 0$. Furthermore, ROSCO's generic blade-pitch and DAC tuning capabilities were extended to be automatically called during an optimization within WISDEM.

Desired closed-loop-response natural frequencies and damping ratios of the first derivative of the blade-root out-of-plane bending moments are defined as input parameters for tuning the trailing-edge-flap controller. With this approach, the flap actuator dynamics will represent the controller's attempt to achieve a prescribed behavior. Therefore, different flap designs with the same tuning frequency and damping ratio achieve similar blade-root-bending moment variations through different trailing-edge-flap deflection angles. In order to emphasize trailing-edge-flap characteristics, this study adapted the flap tuning frequency for each of the three flap sizes (5%, 15%, and 25% span) when located at $r/R = 0.825$. For the flap placement parameterizations and optimizations presented in this study, the flap-controller tuning frequencies were kept constant. Because the tuning procedures in ROSCO automatically tune the flap-controller gains in an attempt to achieve the same closed-loop response of the first derivative of the blade-root-bending moment for each flap location, the standard deviation of the flap-deflection angle is a useful and consistent metric to evaluate the effectiveness of different designs. Note that the tuning frequencies were chosen to prescribe reasonable flap behavior within the trailing-edge-flap saturation limits and therefore do not necessarily result in the best reduction of blade-root flap bending moments possible for each flap design.

3. The Big Adaptive Rotor

As part of the BAR project, a 100-m blade was designed for a low-specific-power turbine. This blade was used as a baseline to display the functionality of the new DAC modeling, analysis, and design optimization capabilities. Within the presented modeling framework, the baseline blade

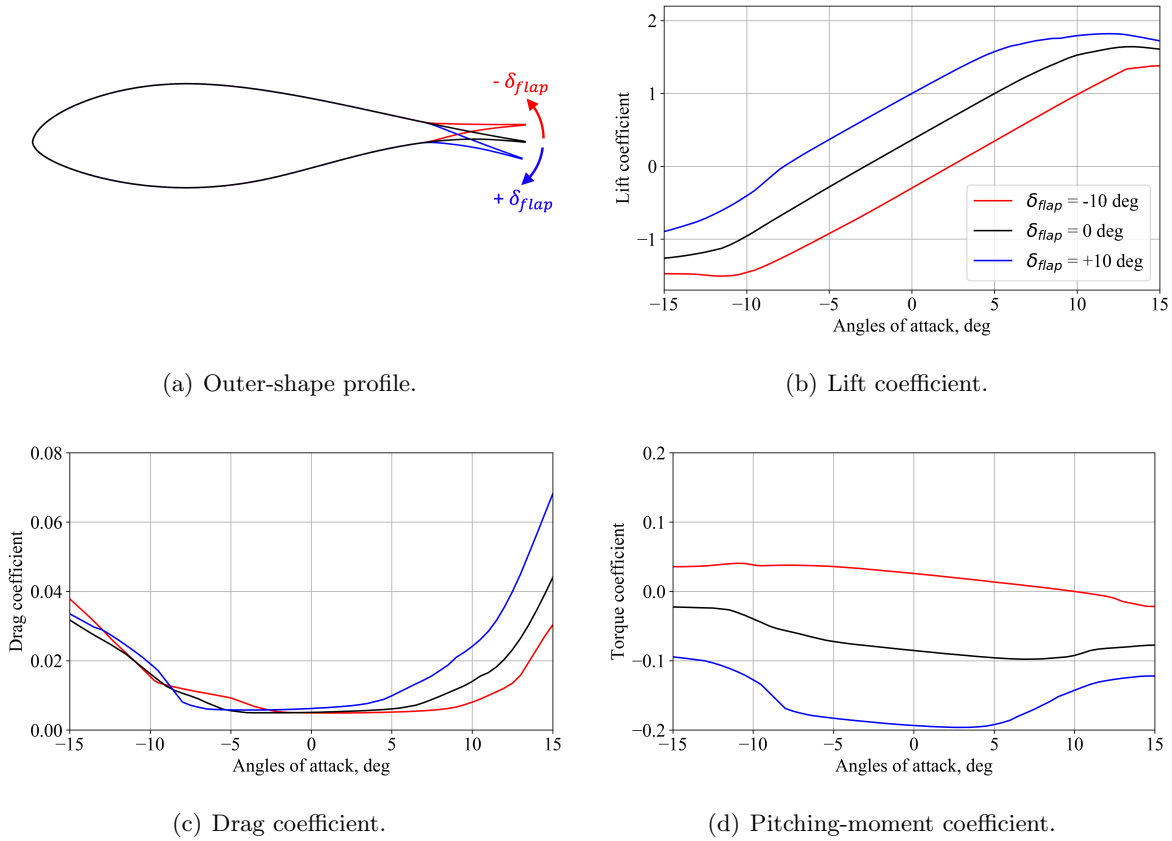

(a) Outer-shape profile.

(b) Lift coefficient.

(c) Drag coefficient.

(d) Pitching-moment coefficient.

Figure 2. Airfoil polar characteristics determined by using XFoil for the FFA-W3-211 airfoil, with and without deflected trailing-edge flaps; blue in downward and red in upward direction.

was modified to include trailing-edge flaps. The basic design parameters of the BAR baseline blade are shown in Table 1. The three-bladed upwind rotor has 100-m blades that each weight approximately 65 tons and have an assumed maximum blade pitch rate of 2°/s. The blades were designed for a tip-speed ratio of 10.5 and to be operated in a low-specific-power turbine of 150 W/m^2. Figure 3 shows the radial distributions of the blades' chord length, twist, and prebend.

The aerodynamic characteristics at specific locations along the radius of the baseline blade were extended to include trailing-edge flaps. For the FFA-W3-211 airfoil outer shape, Fig. 2 shows the resulting airfoil polar characteristics for a trailing-edge flap covering 20% of the blade chord. The trailing-edge flaps' upper and lower deflection limits were set to +10° and -10°. Deflecting the trailing-edge flap by some angle, δ_{flap}, modifies the outer-shape profile (Fig. 2(a)). A positive (downward) deflection results in an increase, and a negative (upward) deflection results in a decrease of the lift coefficient (Fig. 2(b)). Within the linear area, trailing-edge flaps displace the lift curve slope in a quasi-parallel manner. In addition to the intended modification of the lift curve slope, distributed aerodynamic devices also influence respective drag and pitching-moment coefficients (Figs 2(c) and (d)); therefore, modifying the blade aerodynamics to, e.g., alleviate loads, also affects other parameters, such as the rotor's general performance metrics and the blades' elastic deformations.

Table 1. BAR Baseline Rotor Design Parameters.

Parameter	Value/Description
Number of blades	3
Orientation	upwind
Rotor diameter	206 m
Root-cutout length	3 m
Precone angle	4°
Uptilt angle	6°
Airfoil (inboard)	circular
Airfoil (r/R = 0.18)	SNL-FFA-W3-500
Airfoil (r/R = 0.296)	FFA-W3-360
Airfoil (r/R = 0.482)	FFA-W3-301
Airfoil (r/R = 0.765)	FFA-W3-241
Airfoil (r/R = 0.872)	FFA-W3-211
Airfoil (r/R = 1.0)	NACA63-618
Solidity	0.033
Rated wind speed	8.1 m/s
Rated tip-speed ratio	10.5 m/s
Rated rotational speed	7.9 rpm

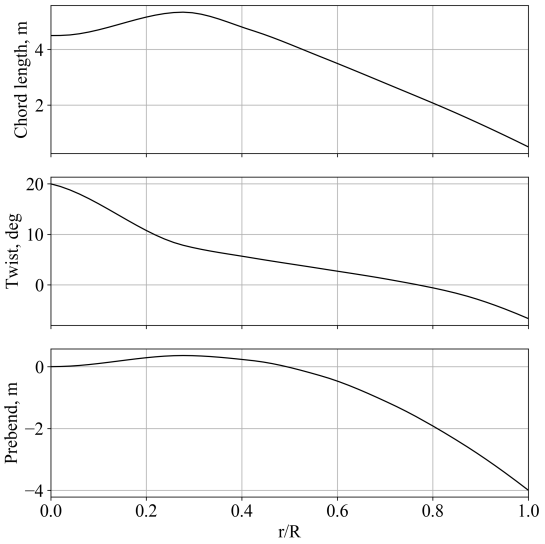

Figure 3. Chord length, twist, and prebend distributions along the blade span for the BAR baseline blade.

4. Results

Based on the BAR baseline rotor blade, three different DAC sizes were evaluated in terms of load alleviation, effectiveness, and other general performance metrics, such as blade-pitch rates and rotor-rotational speed. Results are presented for transient rotor responses in coherent gust and turbulent wind cases. The capabilities of the newly developed modeling and simulation framework are used to conduct trailing-edge-flap placement parameterization and optimization studies, targeting to evaluate DAC design sensitivities and yield optimized DAC placement along the blade span.

4.1. Trailing-Edge-Flap Characteristics

Figure 4 shows aero-servo-elastic transient-domain results of the modified BAR rotor blade with trailing-edge flaps in comparison to the baseline blade without DAC devices. The investigated trailing-edge-flap designs span either 5%, 15%, or 25% of the blade length and cover 20% of the blade chord. Results from Fig. 4 evaluate flaps that were centered at r/R = 0.825. In order to demonstrate the trailing-edge-flap capabilities within the presented modeling framework, desired closed-loop controller responses were chosen for each of the three trailing-edge-flap sizes. Results are analyzed for two different transient wind speed conditions, a coherent gust (Fig. 4(a)), and class A turbulent wind conditions (Fig. 4(b)).

A coherent gust (Fig. 4(a)) presents the general features and benefits of using trailing-edge flaps. Before the gust arose (t < 10 s), the flap-deflection angle was primarily reacting to the 1/rev characteristics of the blade-root flap-bending moments due to wind shear and gravitational effects. When the gust reached the rotor plane, the blade response magnitudes increased and the flaps were deflected to reduce the occurring blade-root flap-bending-moment derivatives. Figure 4(a) shows that the flaps' design can significantly affect the target control objective. A smaller flap has less influence on reducing the control objective. Therefore, within the defined minimum and maximum trailing-edge deflection angles, smaller flaps deflected to greater deflection angles, δ_{flap}, compared to larger flap designs. Because of the modified lift coefficient (Fig. 2(b)) blade-tip elastic deformations, Δx_{tip}, were significantly reduced by targeting to

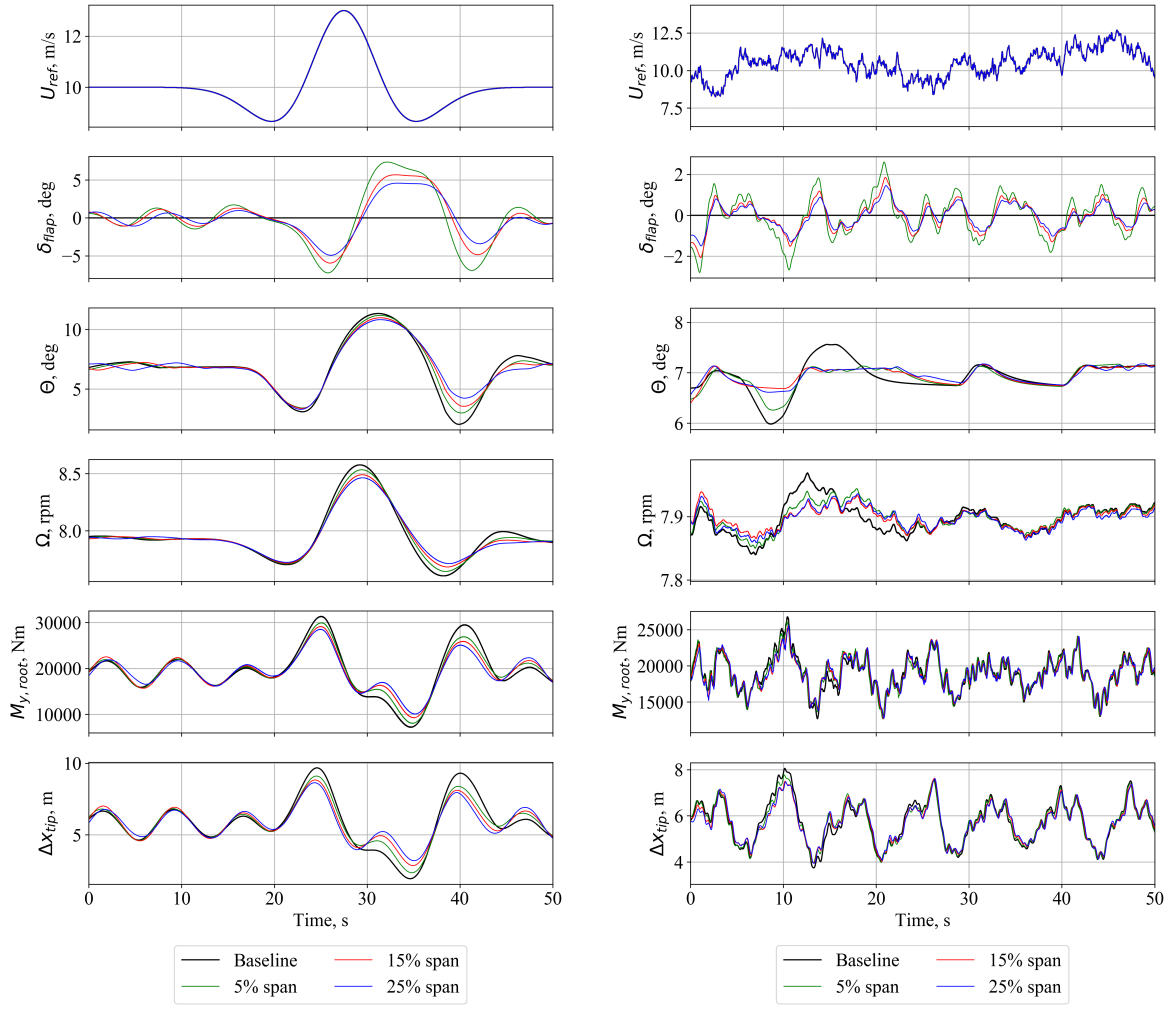

(a) Coherent gust with 3-m/s amplitude (no shear). (b) Class A turbulences at 12-m/s mean wind speed.

Figure 4. Transient results (ref. blade shown) of the BAR rotor equipped with trailing-edge flaps at two different wind speed conditions for the baseline blade and three different flap sizes that have their center located at r/R = 0.825. It shows hub-height wind speeds, U_{ref}; resulting trailing-edge-flap control angles, δ_{flap}; collective blade-pitch angles, Θ; rotor-rotational speeds, Ω; blade-root out-of-plane bending moments, $M_{y,\,root}$; and blade-tip out-of-plane deflections, Δx_{tip}; over time, t.

minimize $\dot{M}_{y,\,root}$. Furthermore, using trailing-edge flaps to mitigate blade loads also resulted in reduced amplitudes of blade-pitch angles and rotor rotational speed. Because of controlling to a constant torque, the rotor power characteristics were equivalent to the rotor rotational speed.

While the coherent gust presents the DAC technology's features and functionalities, the Class A turbulent wind condition with 12-m/s mean wind speed (Fig. 4(b)) shows a more realistic operating condition of a wind turbine. In addition to reducing the standard deviations of the root-flap-bending moment by more than 6%, applying trailing-edge flaps also reduced the blade-tip deflection fluctuations and the blade-pitch angles by up to 8% and 4%, respectively. Furthermore, the impact on rotor-rotational speed and power was beneficial but less pronounced compared to the responses of a coherent gust. Note that these quantities significantly depend

on the automated controller tuning and may further be improved through optimization of the flap-controller tuning parameters or manual tuning of the controller, specifically.

4.2. Design Parameterization and Optimization

By conducting parametric studies, Fig. 5 shows analysis results for the design sensitivity to various flap center locations along the blade span for three flap lengths: 5%, 15%, and 25% span. Furthermore, it presents the optimized flap placement result for each flap size (Fig. 5, symbols framed in black). The prescribed controller tuning parameters for each flap size were adapted to achieve reasonably good reductions of the root-flap-bending moments (Fig. 4) and–for the purpose of an initial comparison–were kept consistent for various flap placements. Note that this controller formulation encourages similar root-flap-bending moment behavior for different flap placements. The underlying design optimization process followed the scheme in Fig. 1 and optimized the flap placement to achieve a minimal standard deviation of the flap-deflection angle as figure of merit.

As expected, larger trailing-edge flaps showed better potential to mitigate blade loads. However, this result is strongly dependent on the actual controller tuning. This study kept such tuning settings consistent, and the resulting flap placements are optimized locations along the blade span for a given flap length. When the trailing-edge flap was located further radially outboard along the blade, modifying the airfoil lift-curve slopes (Fig. 2(b)) was more effective. Trailing-edge flaps yielded a maximum influence at the radial location where the greatest thrust was being generated. Therefore, the optimization resulted in a best flap placement to be near 80% of the blade radius (Fig. 5), which was in accordance with the highest thrust per unit span (Fig. 6). This study revealed that, for the investigated blade, the optimization space for flap placement along the blade span was relatively flat, i.e., it was not sensitive to small placement variations, at least within the outermost 40% of the blade span. Because of smaller thrust levels at the blade tip or further inboard from the peak, increasing the span-wise coverage of the trailing-edge flap with the center being placed in the optimum had a nonlinear increasing benefit on the DAC devices' efficiency. Therefore, the 5% flap already showed a good performance in comparison to the larger flaps.

5. Conclusions

This work discusses characteristics of distributed aerodynamic control devices for large wind turbine rotors. Recent efforts for developing an advanced multidisciplinary modeling environment that combines the capabilities of multiple tools, including OpenFAST, WISDEM, ROSCO, and XFoil, are presented. The approach is well suited to analyze and optimize arbitrary DAC devices and enables comprehensive codesign studies. This work focuses on presenting the newly developed modeling capabilities and evaluates different trailing-edge-flap designs and locations along the radius of the modified BAR baseline blade. The following specific conclusions have been drawn:

- Within a numerical optimization framework, introducing automated controller tuning methods for a specific blade and DAC design was essential to evaluate performance characteristics of DAC devices. To enable DAC optimization, the current workflow is embedded in WISDEM and automatically tunes the pitch and trailing-edge-flap controller.
- The conducted parameterization and optimization studies showed that a specific flap design's ability to achieve a desired control objective peaked at the radial station of maximum thrust per unit span.
- The area of optimal flap placement along the blade span was relatively flat and therefore not sensitive to small placement variations within the outboard 40% of the blade.

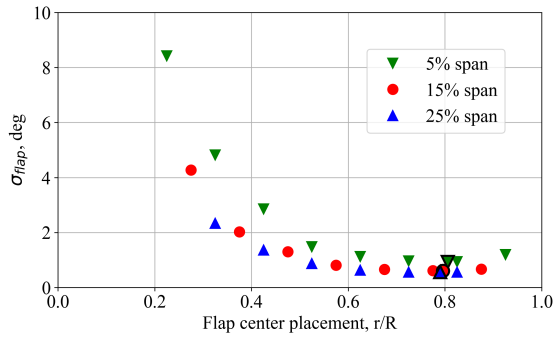

Figure 5. Comparison of trailing-edge-flap design characteristics in terms of the standard deviations of the flap-deflection angle, σ_{flap}.

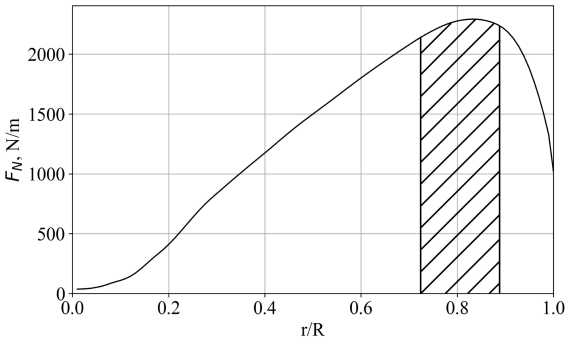

Figure 6. Thrust per unit length distribution, F_N, along the blade span at rated rotor-rotational speed.

- In general, larger flaps had a greater influence on the control objective. The characteristics between different sizes were nonlinear and depended on the load distribution along the blade span, i.e., the amount of thrust that is being manipulated.
- DAC devices were found effective in mitigating loads during both coherent gusts and turbulent wind. This helped mitigate the detrimental effects of slow blade-pitch rates that affect modern large rotors.
- Incorporating DAC devices can be used to improve system-wide performance metrics. The reduction of extreme and fatigue loads on the blade itself, as well as for associated components, such as the pitch-control system, has a large potential to help lower LCOE.

In conclusion, the established modeling environment is well suited to investigate DAC devices for wind turbine application. Future work includes further improvements of the modeling capabilities by accounting for, e.g., different DAC devices, effects on the blade-structural dynamics when integrating trailing-edge flaps, and optimizing the controller tuning parameters. By developing cost functions, including reliability implications, to address the increased complexity and varying blade structure with integrated DAC devices, conducting codesign optimization studies over a range of design load cases, the established modeling environment will furthermore be applied to analyze the impact on the blade's design when using optimized DAC devices and to evaluate its potential for lowering LCOE. The current work on the design and controllability of DAC devices intends to further the understanding of such technologies, and therefore will support mitigating the challenges of current and future wind turbines that incorporate increasing blade length and flexibility.

6. Acknowledgements

This work was authored (in part) by the National Renewable Energy Laboratory, operated by Alliance for Sustainable Energy, LLC, for the U.S. Department of Energy (DOE) under Contract No. DE-AC36-08GO28308. Funding was provided by the U.S. Department of Energy Office of Energy Efficiency and Renewable Energy Wind Energy Technologies Office. The views expressed in the article do not necessarily represent the views of the DOE or the U.S. Government. The U.S. Government retains and the publisher, by accepting the article for publication, acknowledges that the U.S. Government retains a nonexclusive, paid-up, irrevocable, worldwide license to publish or reproduce the published form of this work, or allow others to do so, for U.S. Government purposes.

References

[1] Bolinger, M., Lantz, E., Wiser, R., Hoen, B., Rand, J., and Hammond, R., "Opportunities for and challenges to further reductions in the "specific power" rating of wind turbines installed in the United States," *Journal of Wind Engineering*, 2020. doi: 10.1177/0309524X19901012
[2] Bergami, L., and Poulsen, N.K., "A smart rotor configuration with linear quadratic control of adaptive trailing edge flaps for active load alleviation," *Journal of Wind Energy*, Vol. 18, pp. 625–641, 2015. doi: 10.1002/we.1716
[3] Bergami, L., "Smart rotor modeling," *Springer International Publishing Switzerland*, 2014. doi: 10.1007/978-3-319-07365-1
[4] Pechlivanoglou, G., "Passive and active flow control solutions for wind turbine blades," Doctoral Thesis, University of Berlin, 2013. doi: 10.14279/depositonce-3487
[5] Barlas, T.K., and Kuik, G., "Review of state of the art in smart rotor control research for wind turbines," *Journal of Progress in Aerospace Sciences*, Vol. 46, No. 1, 2010, pp. 1–27. doi: 10.1016/j.paerosci.2009.08.002
[6] Johnson, S.J., Baker, J.P., Van Dam, C.P., and Berg, D., "An overview of active load control techniques for wind turbines with an emphasis on microtabs," *Journal of Wind Energy*, Vol. 13, No. 2-3, pp. 239–253, 2010. doi: 10.1002/we.356
[7] Ai, Q., Weaver, P.M., Barlas, T.K., Olsen, A.S., Madsen, H.A., and Andersen, T.L., "Field testing of morphing flaps on a wind turbine blade using an outdoor rotating rig," *Journal of Renewable Energy*, Vol. 133, pp. 53–65, 2019. doi: 10.1016/j.renene.2018.09.092
[8] Abbott, I.H., and Von Doenhoff, A.E., "Theory of wing sections: Including a Summary of Airfoil Data," *Dover Publications*, 1958.
[9] Bernhammer, L.O., "Smart Wind Turbine: Analysis and Autonomous Flap," Doctoral Thesis, Delft University of Technology, 2015. doi: 10.4233/uuid:b91d9697-d800-417b-bb7e-c5adb00c5e2b
[10] Bergami, L., and Gaunaa, M., "Analysis of aeroelastic loads and their contribution to fatigue damage," *Journal of Physics: Conference Series*, Vol. 555, pp. 1–11, 2014. doi: 10.1088/1742-6596/555/1/012007
[11] Castaignet, D., Barlas, T., Buhl, T., Poulsen, N., Wedel-Heinen, J., Olesen, N., Bak, C., and Kim, T., "Full-scale test of trailing edge flaps on a Vestas V27 wind turbine: active load reduction and system identification," *Journal of Wind Energy*, Vol. 17, pp. 549–564, 2014. doi: 10.1002/we.1589
[12] Ng, B., Hesse, H., Palacios, R., Graham, J., and Kerrigan, E., "Aeroelastic state-space vortex lattice modeling and load alleviation of wind turbine blades," *Journal of Wind Energy*, Vol. 18, pp. 1317–1331, 2015. doi: 10.1002/we.1752
[13] Zhang, M., Yu, W., and Xu, J., "Aerodynamic physics of smart load control for wind turbine due to extreme wind shear," *Journal of Renewable Energy*, Vol. 70, pp. 204–210, 2014. doi: 10.1016/j.renene.2013.12.046
[14] Smit, J., Bernhammer, L.O., Navalkar, S., Bergami, L., and Gaunaa, M., "Sizing and control of trailing edge flaps on a smart rotor for maximum power generation in low fatigue regimes," *Journal of Wind Energy*, Vol. 19, pp. 607–624, 2016. doi: 10.1002/we.1853
[15] McWilliam, M., Barlas, T., Madsen, H., and Zahle, F., "Aero-elastic Wind Turbine Design with Active Flaps for AEP Maximization," *Journal of Wind Energy Science*, Vol. 3, 2018, pp. 231–241. doi: 10.5194/wes-2017-50
[16] Chen, H., and Qin, N., "Trailing-edge flow control for wind turbine performance and load control," *Journal of Renewable Energy*, Vol. 105, pp. 419–435, 2017. doi: 10.1016/j.renene.2016.12.073
[17] Bernhammer, L.O., van Kuik, G., and De Breuker, R., "How far is smart rotor research and what steps need to be taken to build a full-scale prototype?," *Journal of Physics: Conference Series*, Vol. 555, 2014. doi: 10.1088/1742-6596/555/1/012008
[18] Aubrun, S., Leroy, A., and Devinant, P., "A review of wind turbine-oriented active control strategies," *Journal of Experiments in Fluids*, Vol. 58, 10, 2017. doi: 10.1007/s00348-017-2412-0
[19] NREL, *OpenFAST. Version 2.1.0*, https://github.com/openfast/openfast, 2020.
[20] NREL, *ROSCO toolbox. Version 0.1.0*, https://github.com/NREL/rosco_toolbox, 2020.
[21] NREL, *WISDEM. Version 2.0.0*, https://github.com/wisdem/wisdem, 2020.
[22] Drela, M., "XFOIL: An Analysis and Design System for Low Reynolds Number Airfoils," *Springer Berlin Heidelberg*, 1989, pp. 1–12. doi: 10.1007/978-3-642-84010-4
[23] Gray, J.S., John, T.H., Martins, J.R., Moore, K.T., and Naylor, B.A., "OpenMDAO: an open-source framework for multidisciplinary design, analysis, and optimization," *Journal of Structural and Multidisciplinary Optimization*, Vol. 59, No. 4, pp. 1075–1104, 2019. doi: 10.1007/s00158-019-02211-z